Laser Induced Breakdown Spectroscopy of Diesel Particulate Matter Exhaust Emissions Generated from on Road Diesel Engine: Light Duty Vehicles

Richard Viskup, Christoph Wolf and Werner Baumgartner
Institute of Biomedical Mechatronics, Johannes Kepler University Linz, Altenberger str. 69, 4040 Linz, Austria

Keywords: Laser Induced Plasma, Laser Induced Breakdown Spectroscopy, LIBS, Laser Induced Plasma Spectroscopy, LIPS, Optical Emission Spectroscopy, Particulate Matter, PM, DPM, Soot, Black Carbon, Carbon Black, Diesel Combustion Engine, Engines, Emissions, Diesel Emissions, Diesel Exhaust, Diesel, Diesel Engine, WHO, Air Quality.

Abstract: In this research we apply Laser Induced Breakdown Spectroscopy (LIBS) technique for high resolution spectrochemical analysis of Diesel Particulate Matter - DPM exhaust emissions. DPM has been collected from real, on road - Light - Duty Vehicles, driven by combustion Diesel engine. We have been concerned with the main chemical elements, presents in various type of real Diesel particulate matter. From LIBS measurements, it has been shown, that the plasma electron density can be use for the basic classification of different types of DPM matrices. The excitation temperatures of atoms and ions in plasma can be use for further quantitative analyses of diverse Diesel Particulate Matter. The aim of this study is to reveal the compounds, which are mostly dominant in the Diesel engine exhaust emissions and can affect the overall composition of the DPM. The presence of these elements in exhaust emission may point to different processes, mainly to fuel quality, insufficient engine combustion process, incomplete catalytic reaction, inefficient Diesel particulate filtering technique, or failure of the Diesel engine.

SCIENCE AND TECHNOLOGY PUBLICATIONS

1 INTRODUCTION

Diesel combustion engine driven vehicles are currently failing to follow the Euro 6 vehicle emission standards in real driving environment, due to the strict emission norms (Ntziachristos, 2016; Zacharof, 2016; Commission Regulation EU 2016/646). The current existing emission standards *Euro 6* (Commission Regulation EC 692/2008; Regulation EC 715/2007), *Tier 3* (United States Environmental Protection Agency, Regulations) or *LEV III* (California Environmental Protection Agency), for Diesel engine passenger vehicles are the norms for hydrocarbons, carbon monoxide, nitrogen oxides and for particulate matter (PM) from Diesel exhaust emissions, as the total number of all particles.

However, there are no other emission standards for additional compounds or chemical elements contained in the exhaust gas, Diesel particulate matter, PM, or in the soot formed from the Diesel combustion engine. Even though these chemical elements additional to Carbon, present in the particulate matter, forms very significant fraction of the total DPM or the soot emissions content.

In this research we apply Laser Induced Breakdown Spectroscopy technique (Noll, 2012; Miziolek, 2006; Cremers, 2006) for diagnostics of DPM, formed from combustion Diesel engine exhaust emissions, mainly concerning the detection of main chemical elements presents in various DPM matrices.

Laser Induced Breakdown Spectroscopy is an emerging measurement technique (Hahn, 2012) for rapid qualitative (Noll, 2014) and sensitive quantitative compositional analysis (Fortes, 2013; Wang, 2016) of various forms of materials like solids (Viskup, 2012), liquids (Samek, 2000), gases (Effenberger, 2010), powders (Stehrer, 2009) or nanoparticles (Viskup, 2008).

The aim of this study is to measure the main compounds, that are present in these exhaust emissions and can mostly affect the chemical composition of the DPM. The presence of these elements in exhaust emissions may point to different processes, mainly to insufficient engine combustion

Viskup, R., Wolf, C. and Baumgartner, W.
Laser Induced Breakdown Spectroscopy of Diesel Particulate Matter Exhaust Emissions Generated from on Road Diesel Engine: Light Duty Vehicles.
DOI: 10.5220/0007618203080314
In *Proceedings of the 7th International Conference on Photonics, Optics and Laser Technology (PHOTOPTICS 2019)*, pages 308-314
ISBN: 978-989-758-364-3
Copyright © 2019 by SCITEPRESS – Science and Technology Publications, Lda. All rights reserved

process, unburned Diesel, incomplete catalytic reaction, inefficient Diesel particulate filtering technique, or failure of the Diesel engine.

2 EXPERIMENTAL SECTION

LIBS Setup

For Laser Induced Breakdown, the Nd:YAG solid state laser from Quantel has been used. It has been operated at the fundamental laser wavelength 1064nm with 8.5ns pulse duration and laser energy 300mJ per pulse. The laser radiation has been focused with 10cm focusing lens into the plane solid target surface to create plasma. Optical emission from plasma has been collected perpendicularly via optical telescope into the high resolution Echelle spectrograph model Aryelle Butterfly from LTB Berlin equipped with ICCD detector. Spectrometer consists of two separate spectrographs, one part for UV range from 190nm to 440nm and the second part for VIS optical spectrum in range 440nm to 800nm. Spectral resolution capability is from 3pm to 7pm for VUV part and from 4pm to 8pm for VIS part, thus providing spectral information of a broad spectral range with very high resolution and variability. Optical emission from plasma has been collected from VUV as well as from VIS parts, thus the total spectral window from 190nm to 800nm wavelength has been recorded. The delay time 1μs after the laser trigger and gate width 2μs were always kept constant, as well as all experimental parameters during the measurements. In earlier delay time as 1μs the black body radiation is dominating in laser plasma, while in time later than 3μs the atomic and ionic emissions are decaying. The LIBS emission has been recorded in open air atmosphere under atmospheric pressure and at room temperature.

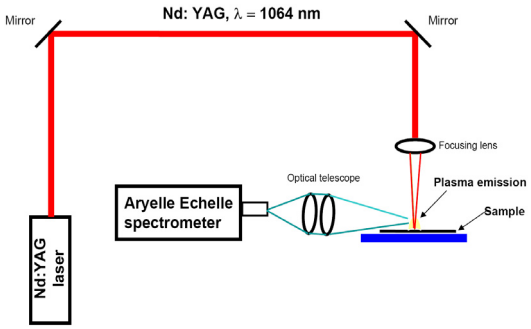

Figure 1: Layout of LIBS experimental setup.

Sample Preparation and Collection

More than 60 different samples from real Diesel engine passenger vehicles of major brand car producers in Europe have been analysed by LIBS. Diesel Particulate Matter has been collected from the tail pipe at the end of the exhaust manifold, after the Diesel Particulate Filter (DPF), if it was applied. Selections of the vehicles were performed randomly and no company was given preference. The results presented here are the selections of eight diverse DPM matrices. Laser induced plasma spectroscopy reveal optical emission lines that are characteristic for UV and VIS spectral region. The collected particulate matter from Diesel engine Light - Duty vehicles exhaust has been mechanically pressed into pellets with flat disc shape. Each displayed LIBS spectrum has been averaged over twelve laser shots.

3 RESULTS AND DISCUSSION

3.1 Identification of the Main Matrix Elements in DPM

Optical emission spectras from Laser Induced Breakdown Spectroscopy measurement of Diesel particulate matter obtained from selected eight matrices, are shown in the Figure 2(a-h).

Diesel particulate matter is characterised by strong optical emission from a) Carbon, b) Iron, c) Magnesium, d) Aluminium, e) Chromium, f) Zinc, g) Sodium and h) Calcium. Spectra shown here are characteristic optical emission lines, dominating in the LIBS spectral signal from 200nm to 800nm.

From figures 2(a-h) it is evident that the chemical composition of selected eight matrices differ considerably from each other. This is due to the different origin of each DPM sample, and due to the unique composition of the exhaust emissions from Diesel engine vehicles. In fact, the source of different compositions is the combination of the Diesel fuel quality, composition of the intake air, quality of the combustion process, type of the engine, or performance of the engine. Other parts that influence the total composition of DPM are applied aftertreatment devices, like Diesel particle filters (DPF) or catalysts like Selective Catalytic Reduction devices. All count to the final chemical composition of DPM.

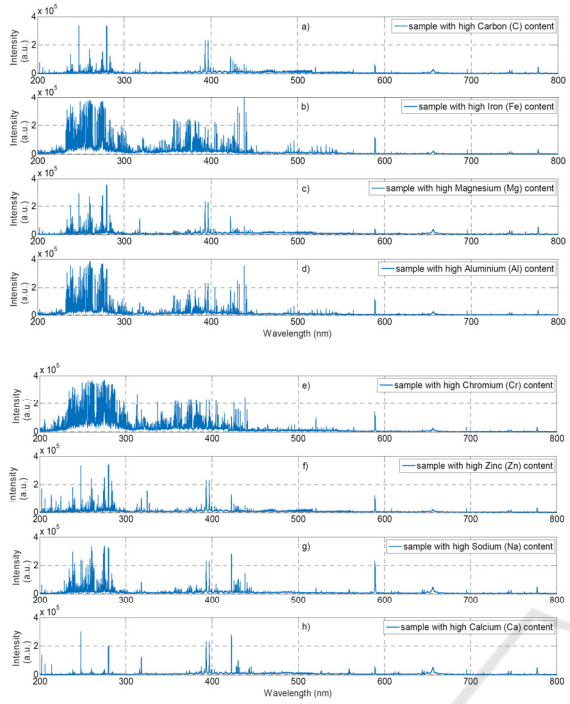

Figure 2: Optical emission spectras generated from Diesel particulate matter measured by high resolution laser induced plasma spectroscopy shows high content of: a) Carbon, b) Iron, c) Magnesium. d) Aluminium, e) Chromium, f) Zinc, g) Sodium and h) Calcium species.

3.2 Comparison of Different Diesel Particulate Matter

From the optical emission spectra shown in the Figure 2(a-h) we selected atomic and/or ionic spectral lines that have a major impact to the line intensity for each Diesel particulate matter matrix. In the Figure 3(a-h) comparison of DPM samples with high measured content of 1. Cr, 2. Ca, 3. Zn, 4. C, 5. Na, 6. Fe, 7. Mg, 8. Al and calculated spectral peak area of: a) Carbon, b) Iron, c) Magnesium, d) Aluminium, e) Chromium, f) Zinc, g) Sodium, h) Calcium - atomic or ionic lines are shown. Here, an individual bar represents calculated peak area of selected spectral atomic or ionic line. These have been obtained after base line correction and calculation of the fitted peak area under the spectral line. From the bar graphs Figure 3, it is possible to obtain relative values of the concentration of chemical elements, presents in the DPM samples. Two types of information can be obtained, by either horizontal or vertical reading of this bar graph.

From horizontal reading of bar graph - Figure 3(a-h) it is possible to observe that Carbon (a) content is not constant in DPM samples, but its concentration rather change in the individual samples (1-8). Iron (b) concentration also varies from low to high in different matrices. Magnesium (c) content is almost always high. Two DPM matrices (6.Fe, 8.Al) posses high value of Aluminium (d). Chromium (e) as well as Zinc (f) content plays important role within the DPM matrices too. Diesel particulate matter contains also Sodium (g) and Calcium (h), and its concentration can be relatively high too.

From vertical reading of this bar graph Figure 3(a-h) it is possible to obtain information about relative concentration of different elements in each DPM matrix. Particularly, sample 1 consists of relatively high level of Iron (b) and Chromium (e). Sample 2: high level of Carbon (a), Zinc (f) and Calcium (h). Sample 3: high level of Carbon (a), Magnesium (c) and Zinc (f). Sample 4: higher level of Carbon (a) and Magnesium (c). Sample 5 relatively high level of Iron (b), Magnesium (c), Sodium (g) and Calcium (h). Sample 6: higher level of Iron (b) and Aluminium (d). Sample 7: higher level of Carbon (a), Iron (b) and Magnesium (c). Sample 8: higher level of Iron (b) and Aluminium (d).

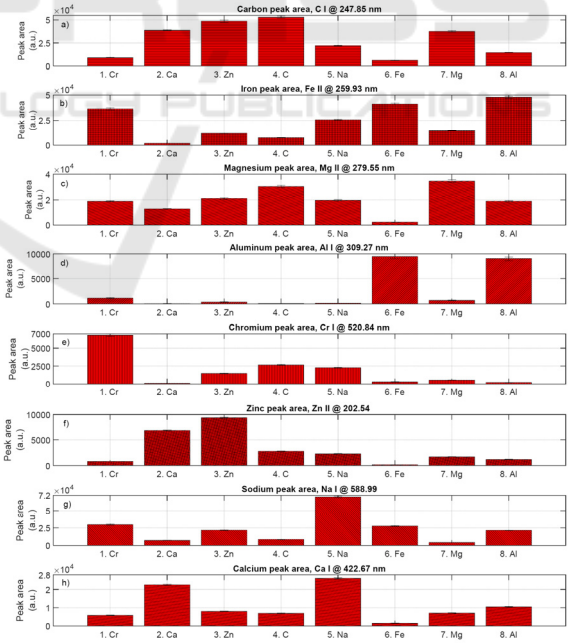

Figure 3: Comparison of eight Diesel particulate matter samples with mostly pronounced content of 1. Cr, 2. Ca, 3. Zn, 4. C, 5. Na, 6. Fe, 7. Mg, 8.Al. Number indicate the sample #, and element name indicate the main element content in DPM matrix.

3.3 Calculation of the Plasma Electron Density

In the case of thermal plasma, and in first approximation, the total width of the line profile mainly depends on electron density (Griem, 1997). Thus a direct measurement of line profile, for which the Stark effect is predominant, leads to electron density, independent of the local thermal equilibrium condition. Calculation of the plasma electron density n_e can be obtained from Stark broadening of H(α) line by applying following formula (Gigosos, 2003):

$$FWHA = 0.549nm \times \left(\frac{n_e}{10^{23}\ m^{-3}} \right)^{0.67965} \quad (1)$$

where FWHA shows the full width high amplitude of the H(α) line broadening at 656.27 nm. Profiles of H alpha spectral lines obtained from individual DPM matrices with high C, Fe, Mg, Al, Cr, Zn, Na, Ca content are shown in Figure 4.

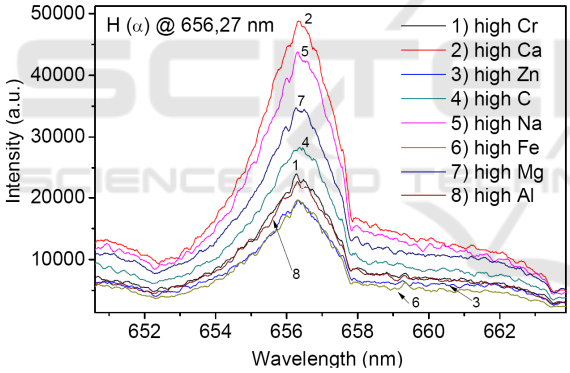

Figure 4: Comparison of H alpha lines for various DPM matrices.

From H(α) line broadening in the Figure 4 and equation (1), the electron concentration n_e has been calculated in interval from 6.6 x 10^{17} cm^{-3} to 8.1 x 10^{17} cm^{-3}. Highest electron concentration n_e = 8.11 x $10^{17}cm^{-3}$ and n_e = 7.97 x $10^{17}cm^{-3}$ has been obtained from sample with high content of Calcium and Sodium respectively. Moderate electron density from plasma were measured in samples with high content of Magnesium n_e = 7.46 x $10^{17}cm^{-3}$, Carbon n_e = 7.49 x $10^{17}cm^{-3}$, Aluminium n_e = 7 .39 x $10^{17}cm^{-3}$, Iron n_e = 7.07 x $10^{17}cm^{-3}$ and Chromium n_e = 7.22 x $10^{17}cm^{-3}$. Low electron concentration in plasma was obtained from sample with high content of Zinc n_e = 6.62 x $10^{17}cm^{-3}$. The comparison of reached electron density in laser induced plasma from Diesel particulate matter is shown in Figure 5.

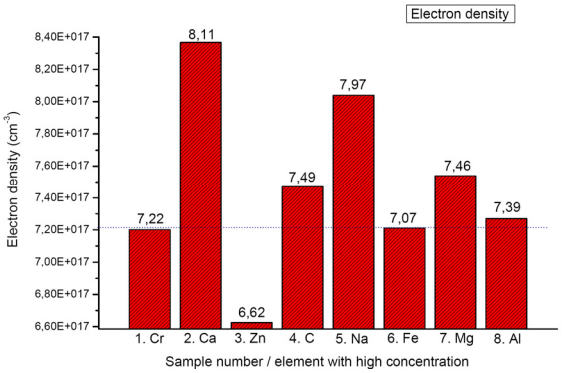

Figure 5: Comparison of electron density n_e from laser produced plasma obtained from eight different DPM matrices. (numbers shown in bar graph are in 10^{17} cm^{-3}).

From the Figure 4 and 5 we can observe that Diesel particulate matter respond to the same laser irradiation conditions with different electron density. This point to distinct type of plasma property for each DPM matrix. However, very similar value of electron density has been measured in case of 1.Cr, 6.Fe and 8. Al samples (shown with dotted line in Figure 5). These are the samples, with measured high concentration of Fe content. Here we can conclude that electron density in laser-produced plasma is alternating according to the matrix type and chemical composition of DPM. Therefore, it can be use for basic classification of different DPM matrices.

3.4 Calculation of the Excitation Temperature

If we assume the local thermal equilibrium in laser plasma, excitation temperature T_{exc} can be obtained from the slope of the Boltzmann plot by calculating the ratio of the relative atomic line intensities, emitted from different excited energetic levels by using the following formula:

$$\ln\left(\frac{I_\lambda^{ul}}{g_{i,u}.A_{ul}.h.\nu_{ul}}\right) = \ln\left(\frac{F.n_i}{Z_i(T)}\right) - \frac{E_{iu}}{kT_{exc}} \quad (2)$$

where $I_\lambda^{u,l}$ is optical emission line intensity, $g_{i,u}$ is the statistical weight of the upper excited state of the chemical species i, $A_{u,l}$ is the corresponding transition probability per unit time, h is the Planck's constant; $\nu_{u,l}$ is the frequency of the photons emitted due to transition from upper excited level u to the

lower level *l*; *F* is the factor depending upon experimental setup; n_i is the concentration of the chemical species *i*; Z_i is the partition function of the chemical species *i* calculated at T_{exc} , $E_{i,u}$ is the energy of the upper excited state of the chemical species *i*; *k* is the Boltzmann constant. For calculation of excitation temperature T_{exc} the background corrected relative intensity of iron atomic lines, emitted at three different excited energetic levels have been used. In Table 1 spectroscopic parameters of atomic iron used for construction of Boltzmann plot are given. Data have been obtained from NIST atomic spectra database (Kramida, 2015). In Figure 6, different Boltzmann plots for DPM samples with high content of Cr, Zn, Na, Fe, Mg and Al are shown.

Table 1: Spectroscopic parameters used for Boltzmann plot.

spectrum	λ_{lu} (nm)	A_{ul} (10^7 s^{-1})	E_l (eV)	E_u (eV)	g_l	g_u
Fe I	364.78	3.38	0.9146	4.3124	9	11
Fe I	374.82	0.915	0.1101	3.4169	3	5
Fe I	407.17	7.64	1.6078	4.6520	5	5

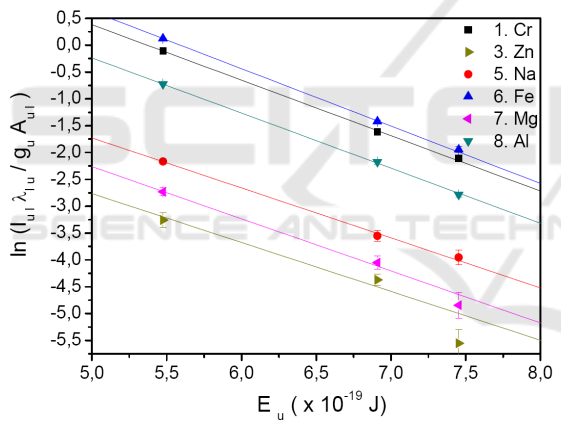

Figure 6: Boltzmann plots and linear fit for determination of T_{exc} for Iron atoms, from DPM samples with high Cr, Zn, Na, Fe, Mg and Al content.

From Boltzmann plot, in Figure 6 we can observe that one sample with increased Zinc content (3. Zn), data point lie outside of the linear curve. This is due to the relatively weak iron spectral line, measured at this wavelength. With lower concentration of iron species in this sample, the spectral line intensity decreases and became less pronounced. Therefore, it was not possible to construct the Boltzmann plot and calculate the excitation temperature for the 2. Ca and 4. C sample, where the concentrations of iron species are even lower. It would be necessary to consider different spectral lines. Figure 7 shows the comparison of plasma excitation temperatures obtained for iron atoms from DPM samples. From the linear fit and slopes of the Boltzmann plots, plasma excitation temperature T_{exc} for Fe atoms has been calculated in interval from 6774 K to 7953 K. Samples with higher concentration of Fe species have lower excitation temperature e.g. T_{exc} (6. Fe) = 6774 K compared to samples with low concentration of Fe, where temperature needed for excitation of these atoms was T_{exc} (3. Zn) = 7953 K. The excitation temperature of Fe atoms in plasma is related to the Iron concentrations in the Diesel Particulate Matter. Therefore T_{exc} parameter can be use for quantitative measurements of DPM. However calculation of the Boltzmann plots and calibration functions are necessary preconditions for each element present in the DPM matrix.

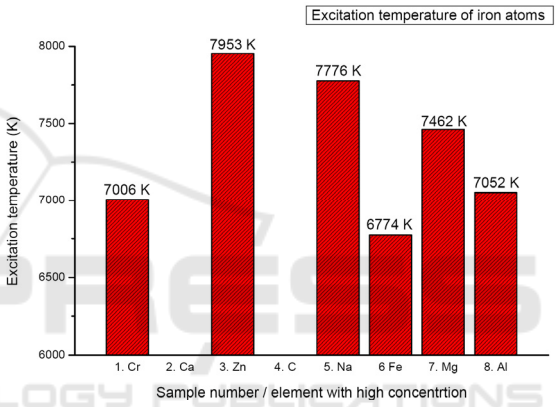

Figure 7: Comparison of the calculated excitation temperature of iron atoms from eight DPM matrices with high measured Cr, Zn, Na, Fe, Mg and Al content.

4 CONCLUSIONS

We have performed laser induced breakdown spectroscopy (LIBS) measurements from more than 60 different samples of Diesel Particulate Matter. DPM were obtained from real, on road - Light - Duty Diesel engine vehicles. Selections of on road passenger vehicles were performed randomly from major brand car producers in Europe. We found that DPM does not consist of purely / mainly carbon particles. However DPM contains many additional compounds - chemical elements with various concentrations. Indeed, we can classify Diesel Particulate Matter into samples with high concentration of Carbon, Iron, Magnesium, Aluminium, Chromium, Zinc, Sodium and Calcium content. These elements, form major compounds of DPM matrix. With the use of laser induced

breakdown spectroscopy, we can very precisely measure elements that are majorly presents in different DPM. The major compounds that are well presents in the DPM are Carbon, Magnesium, Sodium and Calcium. The other major compounds that are also presents in the DPM are Iron, Aluminium, Chromium and Zinc. The concentrations of these elements are changing according to the Diesel engine vehicle. In this paper, quantitative elemental analysis of DPM was not an object. Instead rather qualitative, showing the major chemical elements of different DPM matrices. We have shown individual LIBS spectra's from eight matrices. These are characterised with high concentration of C, Fe, Mg, Al, Cr, Zn, Na and Ca content. We have shown the basic laser plasma properties obtained from various DPM matrices, and we found that electron density n_e in laser induced plasma varies according to the DPM matrix. Therefore it can be use for basic classification of different types of DPM. This has been confirmed by the calculating of the excitation temperature T_{exc} of iron atoms in DPM plasma from Boltzmann plots. The excitation temperatures of atoms and ions in plasma can be use for further quantitative analyses of diverse Diesel Particulate Matter.

Here we have revealed the main chemical elements presents in the various DPM matrices. However further research is necessary to obtain detail picture about the quantitative composition of these elements. Understanding the chemical composition of DPM can help to better control the engine, as well as combustion process and thus reduce unwanted emissions generated from Diesel engine vehicles to meet future environmental emission standards.

ACKNOWLEDGEMENTS

Authors would like to thank to the Austrian Science Fund - FWF for providing financial support under the project number [FWF, P 27967]. Additionally authors would like to thank to Dr. Maria Rusnak for the proofreading and for the corrections.

REFERENCES

Ntziachristos, L. et al. 2016. Implications of Diesel emissions control failures to emission factors and road transport NOx evolution, *Atmospheric environment* 141 542-551. doi: 10.1016/j.atmosenv.2016.07.036

N. Zacharof, et al. 2016. Type approval and real-world CO2 and NOx emissions from EU light commercial vehicles, *Energy Policy* 97 540-548. doi: 10.1016/j.enpol.2016.08.002

Commission Regulation (EU) 2016/646. Commission Regulation (EU) 2016/646 of 20. April 2016 amending Regulation (EC), (No 692/2008) as regards emissions from light passenger and commercial vehicles (Euro 6), http://eur-lex.europa.eu/eli/reg/2016/646/oj

Commission Regulation (EC) 692/2008. Commission Regulation (EC) 692/2008 of 18 July 2008 implementing and amending Regulation (EC) No 715/2007 of the European Parliament and of the Council on type-approval of motor vehicles with respect to emissions from light passenger and commercial vehicles (Euro 5 and Euro 6) and on access to vehicle repair and maintenance information, [Online]. Available: http://eur-lex.europa.eu/eli/reg/2008/692/oj

Regulation (EC) No 715/2007. Regulation (EC) No 715/2007 of the European Parliament and of the Council of 20 June 2007 on type approval of motor vehicles with respect to emissions from light passenger and commercial vehicles (Euro 5 and Euro 6) and on access to vehicle repair and maintenance information, [Online]. Available: http://eur-lex.europa.eu/eli/reg/2007/715/oj

United States Environmental Protection Agency, Regulations for Emissions from Vehicles and Engines, Tier 3 Motor Vehicle Emission and Fuel Standards, https://www.epa.gov

California Environmental Protection Agency, Low-Emission Vehicle Program - LEV III, https://www.arb.ca.gov/

Noll R. 2012. Laser-Induced Breakdown Spectroscopy, Fundamentals and Applications, Springer-Verlag Berlin Heidelberg, ISBN 978-3-642-20667-2

Miziolek A. W. et al. 2006. Laser-Induced Breakdown Spectroscopy (LIBS), Fundamentals and Applications, Cambridge University Press, ISBN 978-0-521-85274-6

Cremers D. A., Radziemski L. J., 2006. Handbook of Laser-Induced Breakdown Spectroscopy, John Wiley & Sons Inc, ISBN 978-0-470-09299-6

Hahn D.W., Omenetto N., 2012. Laser-Induced Breakdown Spectroscopy (LIBS), Part II: Review of Instrumental and Methodological Approaches to Material Analysis and Applications to Different Fields, *Applied spectroscopy,* 66 4 (2012) 347-419. doi: 10.1366/11-06574

Noll R. et al. 2014. Laser-induced breakdown spectroscopy expands into industrial applications, *Spectrochimica Acta Part B*: Atomic Spectroscopy, 41–51 doi: 10.1016/j.sab.2014.02.001

Fortes, F.J., et al. 2013. Laser-Induced Breakdown Spectroscopy, *Analytical Chemistry,* 85 2 (2013) 640-669. DOI: 10.1021/ac303220r

Wang Z.Z., et al. 2016. Laser-induced breakdown spectroscopy in Asia, *Frontiers of Physics,* 11 6 (2016) 114213 doi: 10.1007/s11467-016-0607-0

Viskup R., 2012. Single and Double Laser Pulse

Interaction with Solid State – Application to Plasma Spectroscopy, *Nd:YAG Laser*, ed. D.C. Dumitras, InTech, Rijeka, Croatia (2012) ISBN: 978-953-51-0105-5., open access, http://www.intechopen.com/books/nd-yag-laser

Samek O., et al. 2000. Application of laser-induced breakdown spectroscopy to in situ analysis of liquid samples, *Optical Engineering,* 39 8, 2248-2262. doi: 10.1117/1.1304855

Effenberger A. J., Scott J.R., 2010. Effect of Atmospheric Conditions on LIBS Spectra, *Sensors* 10 5 4907-4925. doi:10.3390/s100504907

Stehrer T., et al. 2009. Laser-induced breakdown spectroscopy of iron oxide powder, *Journal of Analytical Atomic Spectrometry* 24 , 973 – 978. doi: 10.1039/b817279j

Viskup R., et al. 2008. Plasma plume photography and spectroscopy of Fe-Oxide materials, *Applied Surface Science,* 255, 5215-5219. doi: 10.1016/j.apsusc.2008.08.092

Griem H. R., 1997. Principles of Plasma Spectroscopy, Cambridge University Press, ISBN 0521619416 .

Gigosos M. A., et al. 2003. Computer simulated balmer-alpha, -beta and -gamma stark line profiles for non-equilibrium plasmas diagnostics, *Spectrochim. Acta, Part B* 58 (2003) 1489-1504.

Kramida, A., et al. 2015. NIST Atomic Spectra Database, National Institute of Standards and Technology, Gaithersburg, MD.

SCITEPRESS
SCIENCE AND TECHNOLOGY PUBLICATIONS